EUMETSAT/ECMWF Fellowship Programme,
1st Year Report

Developments in the assimilation of geostationary radiances at ECMWF

Matthew Szyndel, Jean-Noël Thépaut, and Graeme Kelly

October 2003

Abstract

The behaviour of geostationary clear sky radiance products generated by the EUMETSAT MPEF from Meteosat MVIRI data and the Cooperative Institute for Meteorological Satellite Studies (CIMSS) from GOES imager data is discussed in the context of their utility for improving numerical weather prediction analyses. Recent changes and proposed future changes to the derivation of these products are examined and discussed. Experiments testing the impact of some of these data on the ECMWF Integrated Forecast System (IFS) are presented. The proposed future work of the fellowship is outlined.

1 Introduction

There have been a number of changes to the available geostationary radiance data over the past year. Changes have been made to the way that Meteosat-7 radiances are processed, with the introduction of a new cloud analysis scheme. Changes have been made to the way that Meteosat-5 data are processed to allow for the growing variations in apparent satellite position. This particular change has led to a considerable improvement in the data and consequently the data are now operationally assimilated at ECMWF. Changes have also been made to the data available from the GOES satellite series. GOES-8 has been taken out of service and replaced with GOES-12, the first of the GOES-M series of satellites. GOES-9 has been positioned over the Pacific to replace GMS-5 until MTSAT-1R can be brought into service. The work of this fellowship has allowed data from these instruments to be assimilated, bringing the total number of geostationary instruments used to bring radiance data to the ECMWF model to five, and thus completing the coverage of the tropics.

Meteosat Second Generation (MSG) is undergoing commissioning at the time of writing, and preparations are under way to allow the monitoring of these data when they become available. Close cooperation with EUMETSAT has allowed prototype code to be constructed and tested at ECMWF. This code is in the final stages of preparation.

Sections 2 and 3 detail the monitoring of data from instruments on board the Meteosat and GOES series of satellites respectively since April 2003. Monitoring prior to this time is covered in Köpken *et al.* 2003. These sections cover both routine monitoring and the monitoring of proposed changes to processing, as well as a short investigation into the impact of a proposed change to RTTOV, the rapid radiative transfer model used by ECMWF (Saunders *et al.*, 1999). Sections 4, 5 and 6 detail assimilation experiments testing the value of data from Meteosat-5, GOES-12 and GOES-9 respectively. Section 7 details an observing system experiment which measures the combined impact of all geostationary radiances within the framework of the latest operational model at ECMWF. Finally section 8 summarises and details future plans.

2 Meteosat series monitoring

Meteosat-7 clear sky radiance processing changed in June, with a new cloud analysis scheme being implemented. The impact of this change was analysed at ECMWF with a small dataset sent by EUMETSAT prior to implementation. Another change in processing was implemented for Meteosat-5 clear sky radiances in March 2003 to allow far more accurate radiative transfer modeling of the data. The change is to the local satellite zenith angle of each observation, remedying the problem described in Köpken, 2003. Furthermore, two short experiments have been carried out to investigate the impact of a new calibration scheme for Meteosat-7 and a new approach to radiative transfer in RTTOV, the rapid radiative transfer code used by ECMWF. As expected the solar stray light effect continues to be visible in Meteosat clear sky radiance data, particularly in the eclipse season.

2.1 Meteosat-7

Meteosat-7 water vapour radiances continue to exhibit a 3.5 K positive mean bias with respect to radiances modeled from the short range forecast provided by the ECMWF integrated forecast model (IFS) using RTTOV: see figure 1. This bias was unaffected by the introduction of the SCART cloud analysis in June. The standard deviation of the first guess departure of this data also remains static at between 1.2K at the start of the assimilation window and 1.8K at the end of the window, as the error in the first guess increases; see figure 2. This statistic varies slowly over the year between 1.2K and 2.2K.
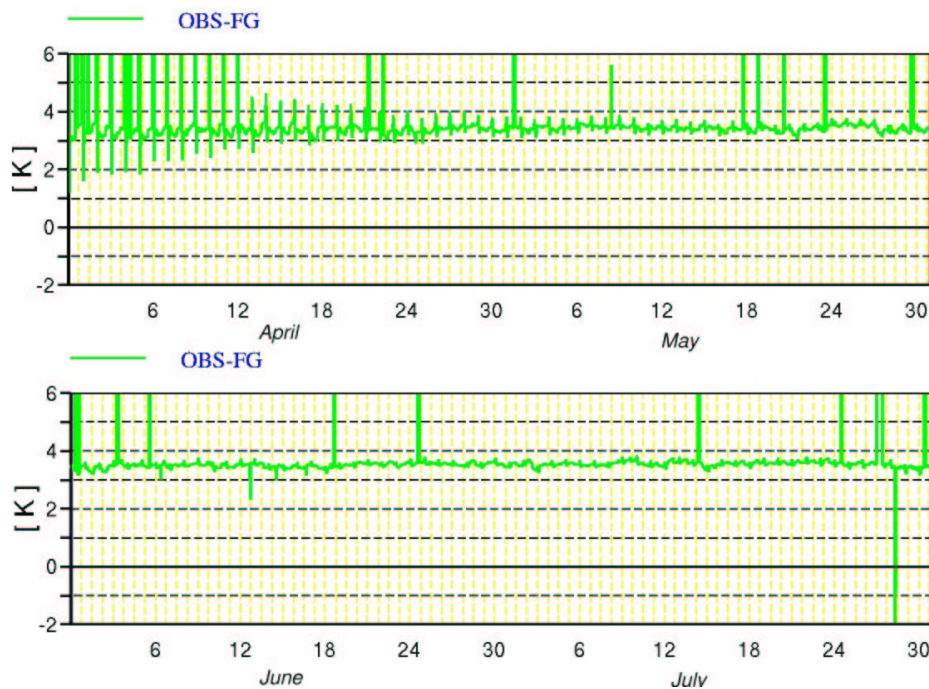
Figure 1: Meteosat-7 water vapour channel first guess departure.

The introduction of the SCART cloud scheme is, however, evident in the infrared window channel radiance data. The following comments all relate to data over the sea to reduce the effects of poor modeling of the land surface temperature diurnal cycle. Prior to the introduction of the SCART cloud scene analysis the mean first guess departure of these data stood at around -3.5K for all data, and -2.8K if only data with 100% clear segments are considered. After the introduction of the SCART analysis the mean bias stands at about -2.8K for all data and about -2.3K for the 100% clear data – see figure 3. All of these IR biases have a diurnal cycle around the mean of around half a degree in amplitude. The reduction in cold bias of these data is consistent with the observation that the SCART cloud analysis scheme diagnoses more pixels as cloudy than the old histogram analysis method (see section 2.4). As a result it is likely that there has been a reduction in the amount of undiagnosed low level cloud in the CSR product, leading to a reduction in the cold bias. A strong diurnal cycle is in evidence in the IR first guess departures, either a result of a poor modeling of the diurnal cycle of surface temperature or as a result of undiagnosed convective cloud. The standard deviation of the first guess departure drops with the introduction of the SCART scheme from around 1.5K to 1K when all data are considered and from around 1K to 0.8K when only data with 100% clear segments are considered – see figure 4. The standard deviation exhibits a diurnal cycle, increasing during the daytime. This diurnal cycle is reduced by the introduction of the SCART scheme.
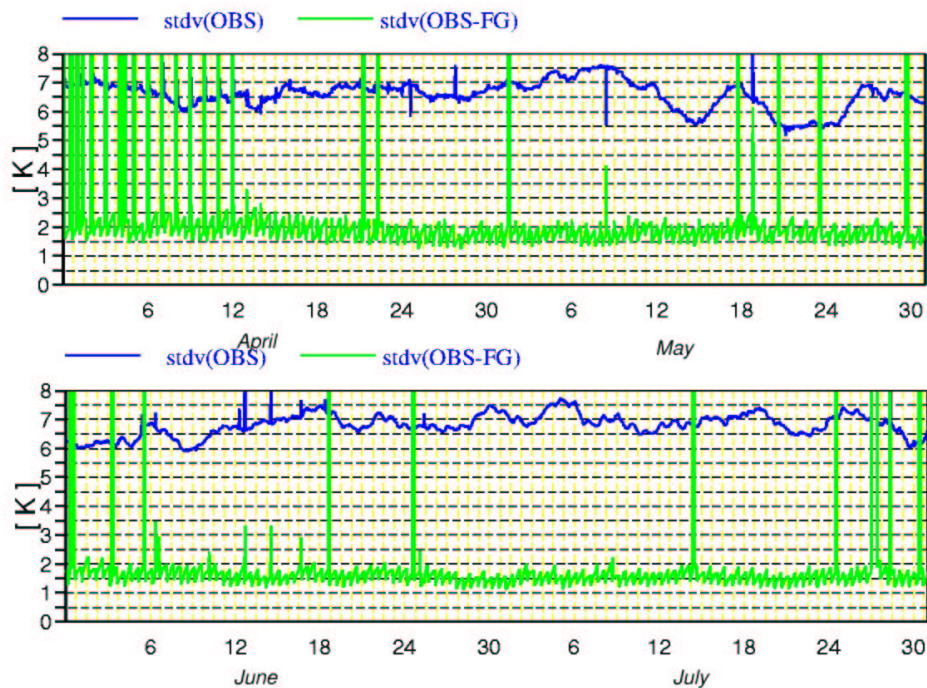
Figure 2: Meteosat-7 water vapour channel first guess departure standard deviation.

2.2 Meteosat-5

On 18th March the processing of Meteosat-5 radiances was altered to update the transmitted local satellite zenith angle more frequently. This change was introduced to remove a latitude dependent diurnal bias identified by Christina Köpken and linked to local satellite zenith angle by Leo van de Berg (Köpken *et al.*, 2003). The implementation of this fix has removed most of this diurnal bias: see figure 5. A small, phase shifted residual bias is still in evidence.

Routine monitoring since the implementation of this fix has shown the Meteosat-5 water vapour channel to be a mean 2.5 - 3K warmer than the IFS first guess implies, with slow variations following the implementation of the fix; see figure 6. As Meteosat-5 data were not assimilated until October 2003 (see below) this slow variation is not unexpected. The standard deviation of the first guess departure also slowly varies, taking values between 1.5K and 2.5K – see figure 7.

Monitoring of the infrared channel of Meteosat-5 over the sea shows a mean bias of around -4K when all data are summed over, and a mean bias of around -3.5K when only 100% clear data are considered – see figure 8. The standard deviation lies around 2K for all data and 1K for 100% clear data – see figure 9.

It is noticeable that the the biases and standard deviations of both channels on Meteosat-5 exhibit different characteristics despite Meteosat-5 being calibrated from Meteosat-7 observations in the mutually observed area. This is still the case when observations are restricted to the mutually observed area, and this phenomenon persists despite the fix of the local satellite zenith angle problem on Meteosat-5. The reason for this remains unclear.
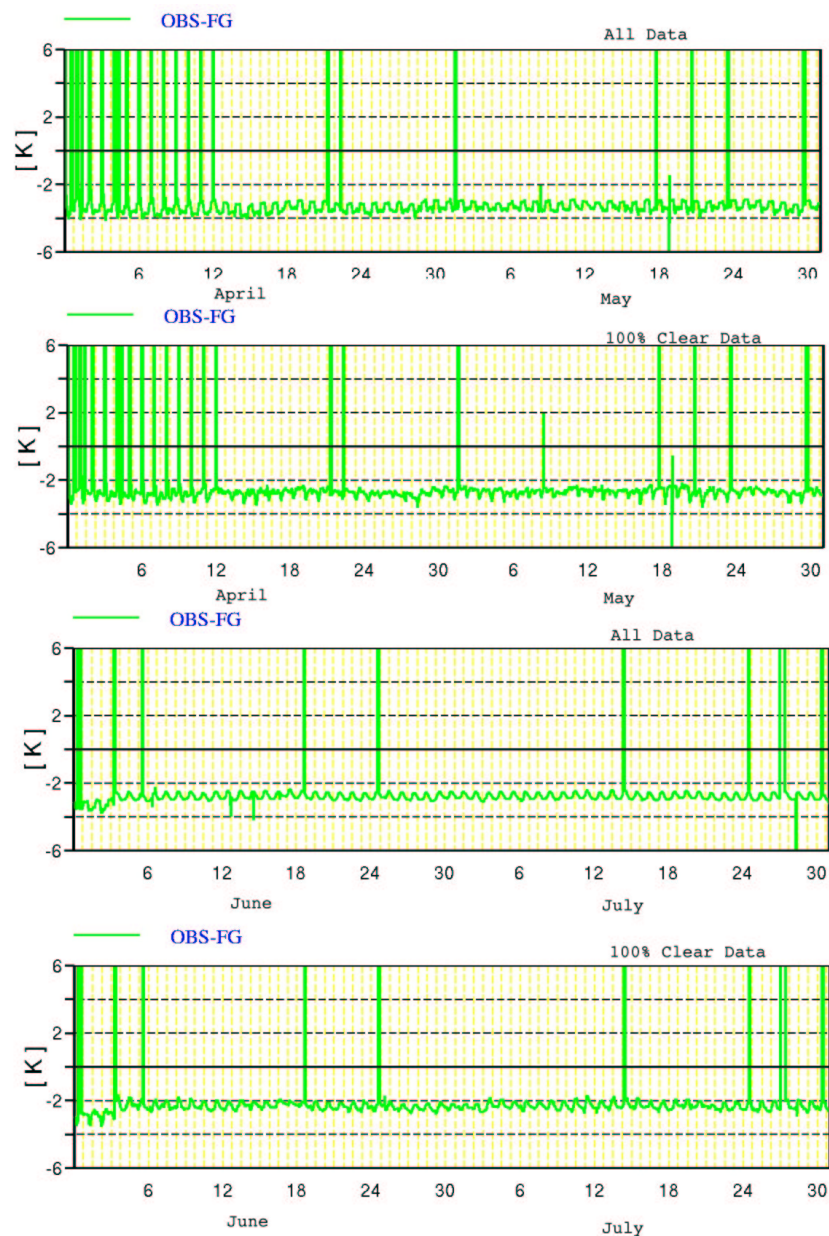
Figure 3: Meteosat-7 infrared channel first guess departure. 1st and 3rd panels show all data while 2nd and 4th channels show only data from 100% clear segments.

2.3   Planck weighted RTTOV

The current formulation of RTTOV makes the assumption that the radiance being modeled is constant across the instrument response function, relying upon the narrow spectral width of satellite channels to make this assumption valid. The water vapour channel on the MVIRI instrument is not narrow, extending from 5.7 to 7.1 μm. It is possible to calculate coefficients for RTTOV which replace the above assumption with an assumption that the radiance is a Planck function. It is to be hoped that radiative transfer based on such a set of coefficients would reduce the mean bias between observations and first guess in the MVIRI water vapour channel.

To test the above conjecture Pascal Brunel (Météo-France, Lannion) prepared a set of RTTOV coefficients for MVIRI on Meteosat-7 and we conducted an experiment to compare the first guess departures using the two
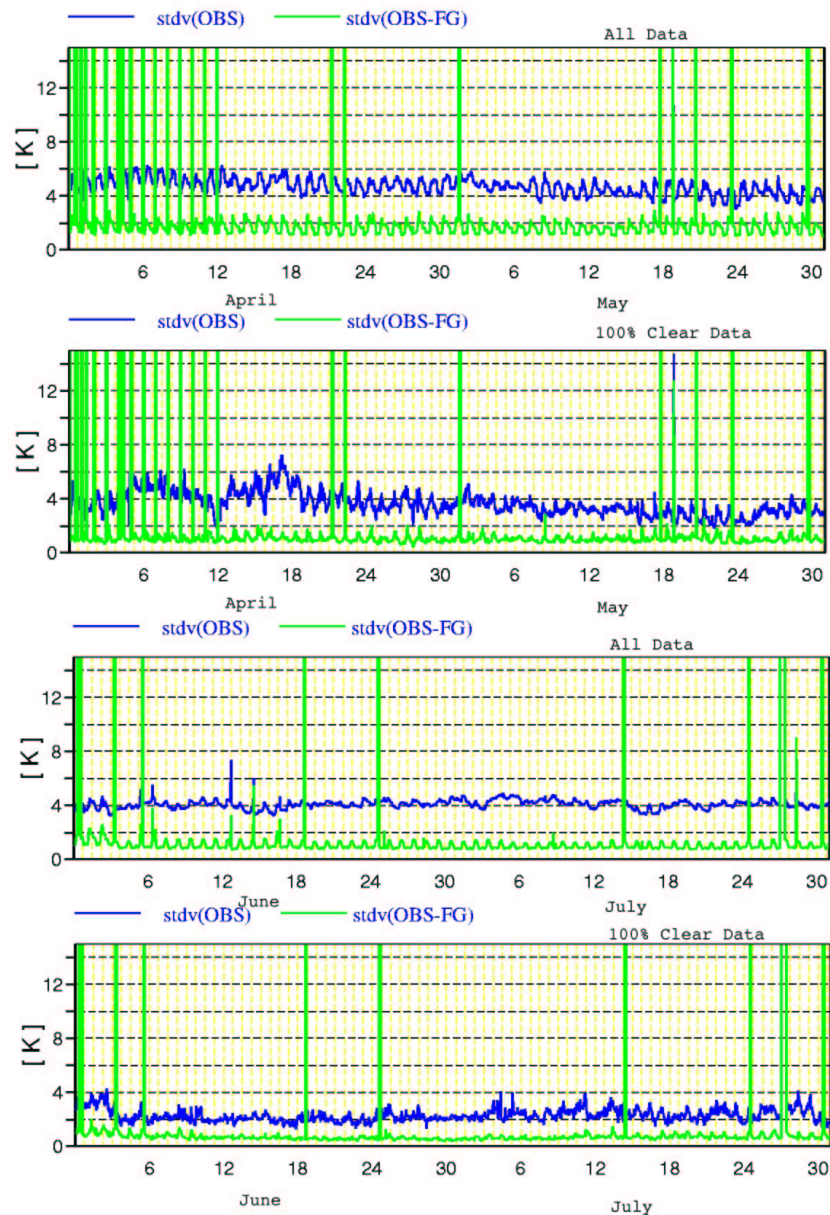
Figure 4: Meteosat-7 infrared channel first guess departure standard deviation. 1st and 3rd panels show all data while 2nd and 4th channels show only data from 100% clear segments.

different methods of calculating the radiances from the model. Meteosat-7 was not assimilated in either the experiment or the control as the altered simulated radiances would lead to different increments. Both were run as T511 4DVAR experiments over the first 3 days of June 2003 using IFS cycle 26r1. Meteosat-5, GOES-10 and GOES-12 were assimilated along with conventional and polar orbiting satellite data.

The results of this limited trial show a reduction in the average first guess departure of around a degree, somewhat larger than the 0.7 degrees previously thought (Christina Köpken, 2002). Figure 10 shows the Met-7 departures in the two experiments. The change in bias over these three days shows only a small amount of geographical variation as shown in figure 11.

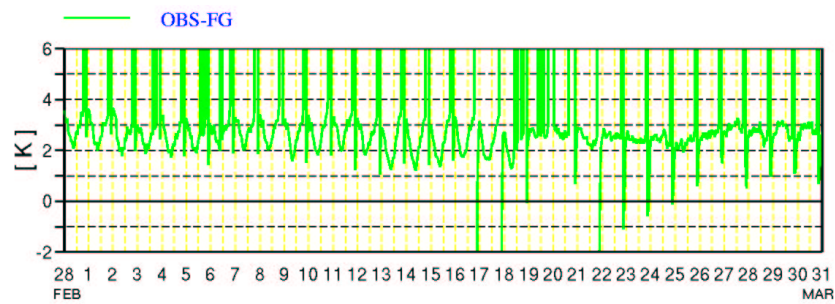This result goes some way toward explaining the large mean first guess departure observed in data from

Figure 5: Meteosat-5 water vapour channel mean first guess departure in the northern hemisphere in March 2003.
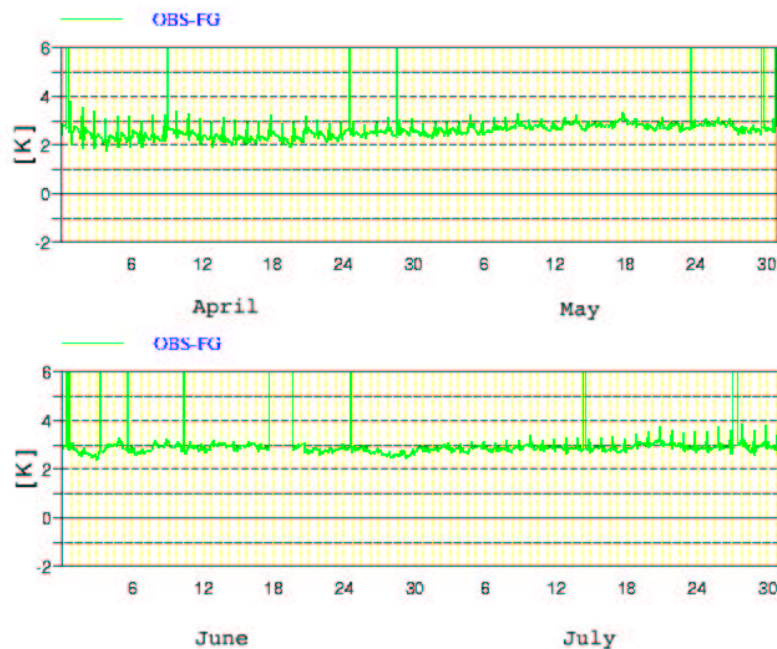

Figure 6: Meteosat-5 water vapour channel mean first guess departure in the northern hemisphere for April to July 2003.

Meteosat-7, Meteosat-5 and GOES-12's water vapour channels.

2.4 SCART cloud scheme and blackbody calibration

As mentioned above a new cloud scene analysis scheme, SCART, was implemented by EUMETSAT on 4th June. The new scheme is a version of the MPEF SEVIRI cloud scheme altered to fit the MVIRI instrument. Prior to the implementation of the SCART scheme we tested a sample of data to diagnose the impact of the scheme on the Meteosat-7 CSR product. After the implementation of SCART it became apparent that the vicarious calibration of MVIRI had diverged from the blackbody calibration. To prevent this divergence new blackbody calibration coefficients were derived by EUMETSAT. The results of this new calibration were also
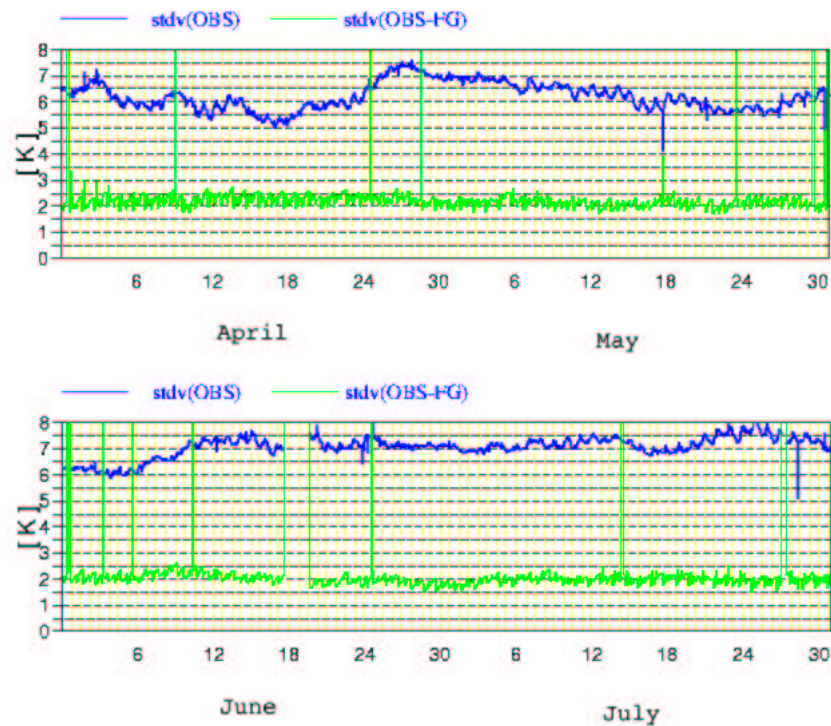
Figure 7: Meteosat-5 water vapour channel standard deviation of first guess departure in the northern hemisphere for April to July 2003.

assessed at ECMWF. At the time of writing the new coefficients are yet to be implemented operationally.

The first test consisted of an experiment and control. The experiments were run using a forecast model of resolution T159 (about 125 km) with a 3DVAR with first guess at appropriate time (3DVAR FGAT) assimilation using IFS cycle 26r1. Both experiments blacklisted geostationary radiances and atmospheric motion vectors (AMVs) to avoid the divergence of the analyses and ran from the 12th May 2003. The water vapour results showed little difference between the two schemes, with the principle change being the amount of cloud diagnosed. An examination of the radiance data showed them to be very similar (not shown). The SCART cloud analysis increases the number of cloudy pixels found in the water vapour; see figure 12. The infrared data also have a greater number of segments flagged as cloudy, but in this case the radiances have also changed. The first guess departures show a reduction in the number of outliers both in terms of a reduction in the standard deviation of first guess departure (particularly between 0600 and 0900 UTC, not shown) and in terms of the number of pixels with large departures in the geographical plot – see figure 13. As the values of water vapour CSRs were largely unaffected the change in cloud scheme had no discernable impact on Meteosat-7 radiance assimilation.

As mentioned above, after the introduction of the SCART cloud scheme it became necessary to alter the blackbody calibration method as the vicarious calibration used to validate the blackbody calibration had started to diverge from the blackbody calibration. Again we were given some test data to allow us to examine the impact of the change in calibration. Again the experiments were run as T159 3DVAR FGAT experiments using IFS cycle 26r1, this time for the first 11 days in August. Once again all geostationary clear sky radiances were excluded, but this time the satellite winds were included, with all winds based on the operational processing. The new calibration had a number of effects. The most obvious effects were that the water vapour channel bias
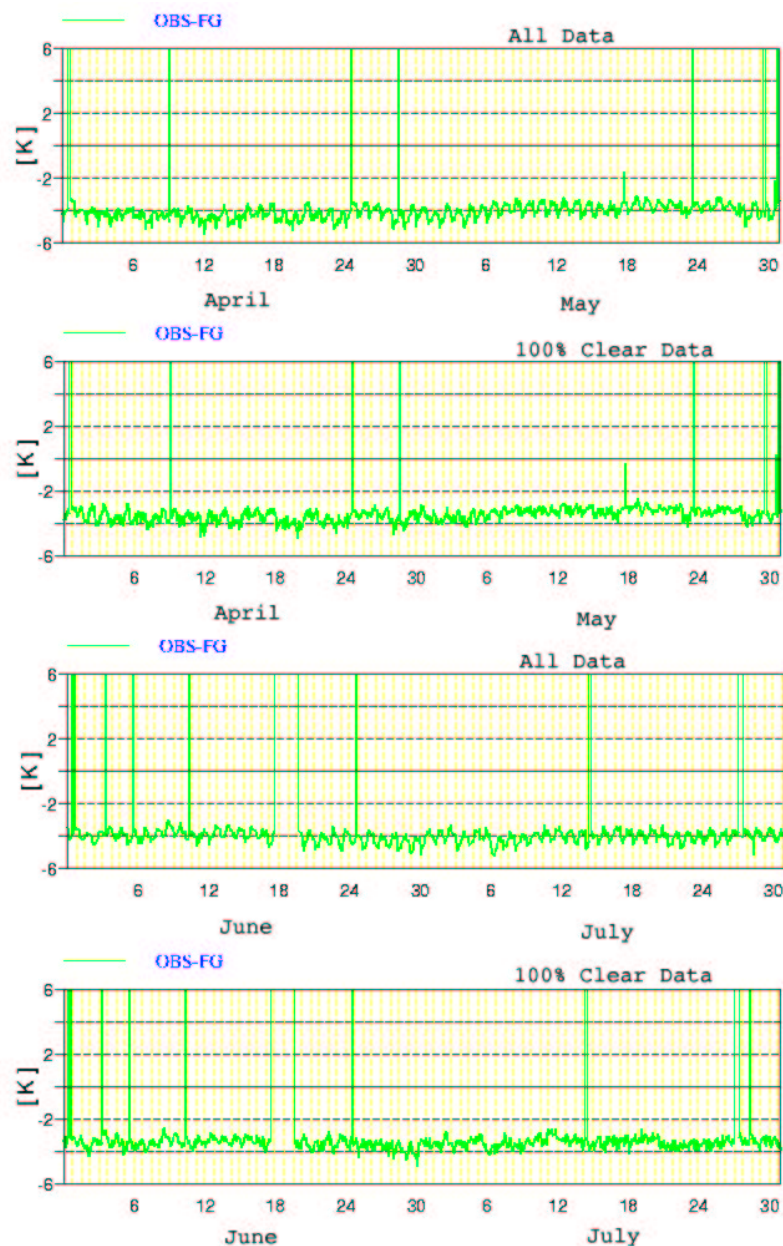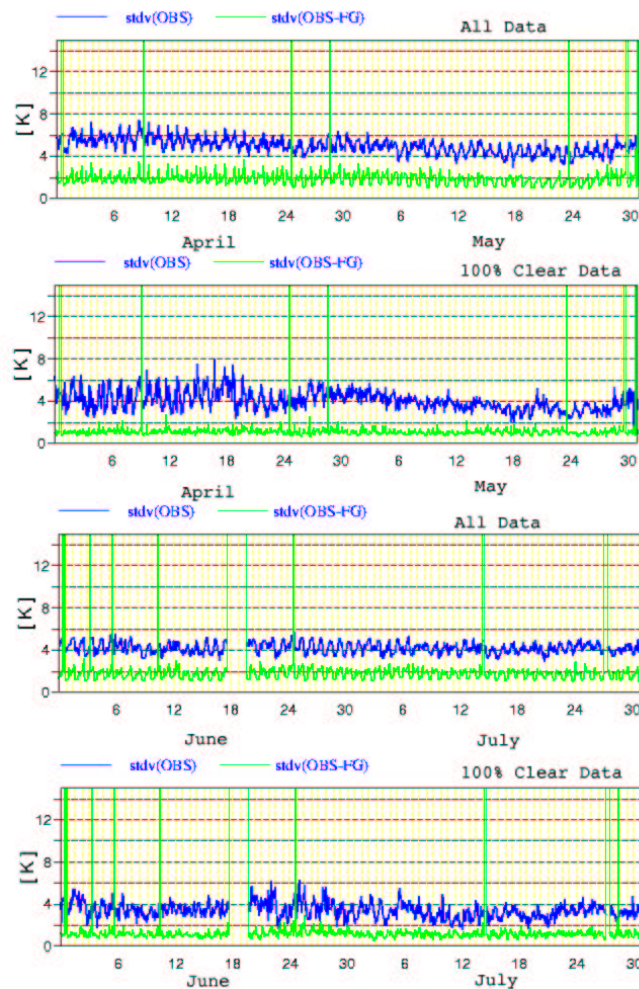
Figure 8: Meteosat-5 infrared channel mean first guess departure in the northern hemisphere for April to July 2003. 1st and 3rd panels show all data while 2nd and 4th channels show only data from 100% clear segments.

was reduced by about 0.5 degrees, and the infrared channel bias was reduced by about 1 degree. However, the introduction of the new calibration does reduce the number of pixels diagnosed as cloudy – see figures 15 and 16. This result shows that at least some of the large mean first guess departure of Meteosat-7 water vapour radiances is due to undiagnosed cloud under the old histogram cloud analysis scheme.

3   GOES series monitoring

Over the period between April and September 2003 two changes have been made to the GOES satellite observing network. On the 1st April GOES-8 was removed from operational service at the 75° west station and

Figure 9: Meteosat-5 infrared channel standard deviation of first guess departure in the northern hemisphere for April to July 2003. 1st and 3rd panels show all data while 2nd and 4th channels show only data from 100% clear segments.

replaced by the GOES-12 satellite. A month later the GOES-9 satellite was brought into service at $140°$ East to cover the Pacific area formerly observed by GMS-5, to act as cover until MTSAT can be replaced.

Figure 17 shows the monitoring statistics for GOES-10 and GOES-12 over August and September for the northern hemisphere. The region is limited to the northern hemisphere to avoid rapid variations in the graph due to the differing schedule of sampling of the southern hemisphere by the GOES scanning pattern. Both instruments show a diurnal cycle, with the cycle in GOES-12 being particularly strong. This diurnal cycle is probably linked to a well documented phenomenon (Köpken et al., 2003, Johnson and Weinreb, 1996) in the GOES series of satellites. These spacecraft are 3 axis stablised, and consequently different parts of the spacecraft are heated by the sun at different times of the day. Around local midnight part of the spacecraft is heated which radiates into the blackbody. As the blackbody is not perfect, some of the radiation is reflected resulting in a cold calibration around local midnight, particularly of shortwave channels like the 3.9μm and 6.7μm channels.

Figure 18 shows the monitoring statistics for GOES-9 over most of September and the beginning of October 2003, charting the mean and standard deviation of the departure of observation from the ECMWF 'esuite', the test bed for a new operational forecast system. The area monitored this time is the southern hemisphere, as the
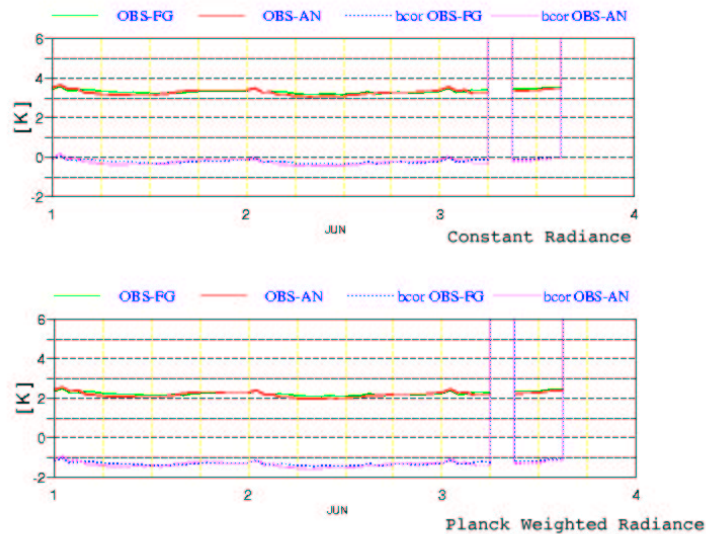
Figure 10: First guess and analysis departures of Meteosat-7 radiances from the IFS as calculated by RTTOV-6M using a constant radiance assumption (top panel, as operations) and a Planck weighted assumption (bottom panel).

northern hemisphere is scanned on a less frequent basis than the rest of the disk. GOES-9 exhibits no obvious diurnal cycle.

GOES-10 exhibits a mean bias against first guess of around 1.2 degrees and has a first guess departure standard deviation of between 1 and 2 degrees. GOES-12 has a mean first guess departure of about 1.7 degrees with a first guess departure standard deviation of between 1.2 and 2.5 degrees. GOES-9 exhibits a constant mean bias of 1 degree, and has a standard deviation of first guess departure of about a degree.

The differing behaviour of GOES-12 from the other two GOES imagers in operational use may in part be linked to the different filter function of the GOES-12 imager water vapour channel. This filter function is considerably broader than that on the earlier GOES imagers (to allow for an increase in spatial resolution), and has a weighting function which peaks lower in the atmosphere. Consequently GOES-12 CSRs are more prone to errors in the lower tropospheric humidity, more likely to see the Earth surface or undiagnosed low cloud and are more sensitive to radiative transfer errors leading from the constant radiance assumption of RTTOV. Finally, as the weighting function extends to shorter wavelengths, the GOES midnight calibration effect is likely to be more severe. For details of the differences between the GOES-12 imager and earlier GOES imagers, see Hillger et al., 2003.

4 Assimilation of Meteosat-5

The improved monitoring statistics for Meteosat-5 have led to the possibility of assimilation. We carried out a 15 day trial to assess the impact of the assimilation of Meteosat-5 water vapour channel clear sky radiances. Meteosat-5 is operationally calibrated from Meteosat-7 radiances in the area viewed by both satellites, and as a consequence it is likely that the radiances from the two instruments in this area are correlated. As a precaution Meteosat-5 radiances east of 40°E are blacklisted. Furthermore data are blacklisted around local midnight to avoid radiances affected by solar stray light. Data over land above 1500 m and with fewer than 70% of the
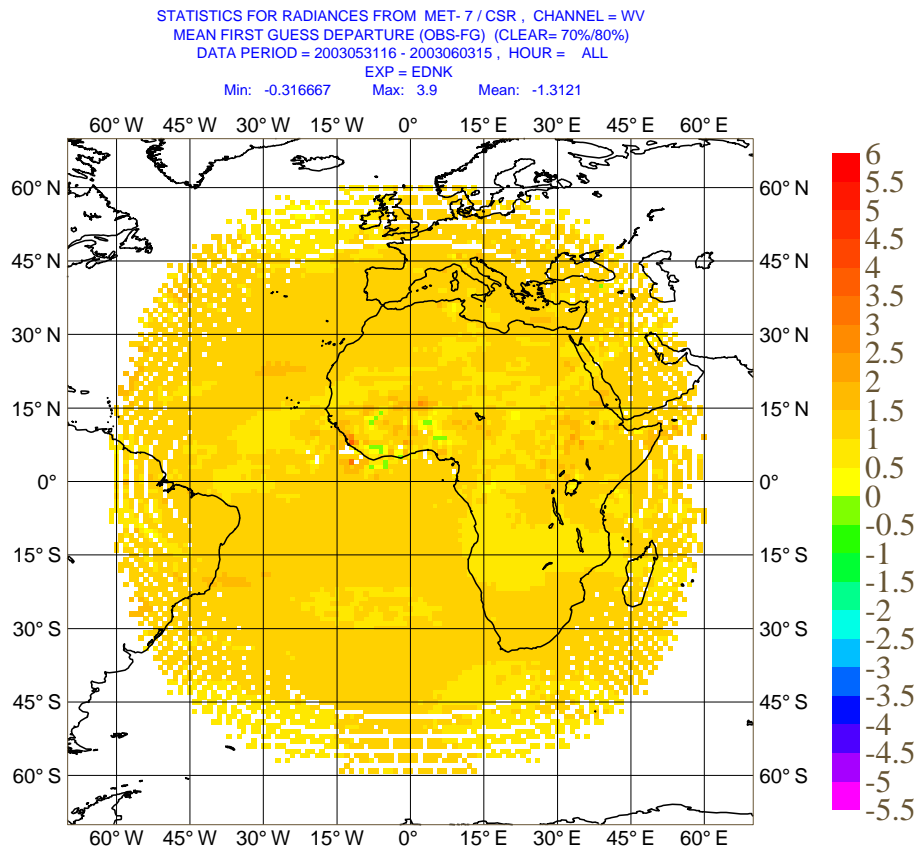
Figure 11: Difference between time averaged first guess departure of Meteosat-7 radiances using flat and Planck-weighted radiance assumptions.
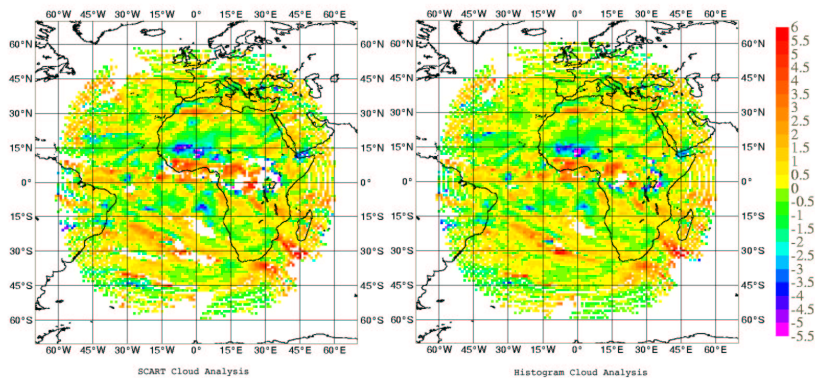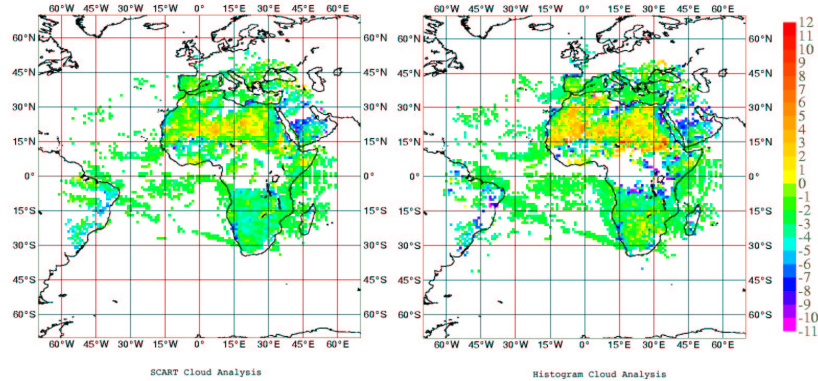

Figure 12: Bias corrected first guess departure of Meteosat-7 water vapour radiances using SCART cloud analysis and histogram cloud analysis over the period 1000 UTC on 12th May 2003 to 0900 UTC 13th May 2003. Note white areas denoting cloudy data.

segment clear of cloud are also not assimilated. Finally, in the past Meteosat-5 data have been observed to be unstable around the eclipse period at times not limited to those around local midnight, and so all Meteosat-5data have been excluded from assimilation during the eclipse season. Subsequent analysis of the September eclipse period 2003 has shown these data to be stable, so previous problems were probably linked to the satellite position problems outlined in Köpken *et al.*, 2003. The blacklist will be relaxed in the future.

Figure 13: First guess departure of Meteosat-7 infrared radiances using SCART cloud analysis and histogram cloud analysis over the period 1000 UTC on 12th May 2003 to 0900 UTC 13th May 2003. Note white areas denoting cloudy data.

The assimilation experiment was run concurrently with an experiment with GOES-12 assimilated to save on computation time. Subsequently an improved bias correction for GOES-12 was deemed necessary and another assimilation experiment run (see section 5), but both experiment and control in this section assimilate GOES-12. The experiment is based upon ECMWF cycle 25R1, the operational IFS over the experiment period of 8th to 22nd April 2003.

Examination of the anomaly correlation of the 300 and 500 hPa geopotential height fields shows the assimilation of Meteosat-5 WV radiances to be of neutral to positive impact, with Meteosat-5 appearing to be slightly ahead in this sample – see figure 19. It should be noted that this experiment has only 15 cases, and is therefore of relatively low significance. An analysis of the RMS errors in the 300 hPa geopotential height field at 48 hours show that the assimilation of Meteosat-5 radiances is beneficial for most areas, although the area west of Australia appears to have a degraded forecast – see figure 20. The impact of the assimilation of Meteosat-5 on the upper tropospheric humidity can be seen by examining the change in RMS first guess departure of HIRS channel 12 on board NOAA-16. This channel is sensitive to upper tropospheric humidity. An area of reduced RMS first guess departure may be seen in the area where Meteosat-5 is assimilated – see figure 21.

As a result of these experiments the decision was taken to assimilate Meteosat-5 WV CSRs. This was reflected in IFS cycle 26r3, which was implemented operationally on 7th October 2003.

5   Assimilation of GOES-12

When GOES-8 was replaced with GOES-12 on 1st April we did not immediately assimilate the GOES-12 data. The GOES-12 imager is the first of the GOES-M series, and has a different channel set to that found on the GOES-8 imager. An assimilation trial seemed prudent. An experiment assimilating GOES-12 WV data was carried out over 22 days, covering the period 13th May to 3rd June 2003. The experiment differed from the control only in the assimilation of GOES-12 data. The control was IFS cycle 26R1, the then operational IFS. The GOES data were assimilated with a slightly different blacklist from the GOES-8 data. Data were still rejected if the local satellite zenith angle was above $60°$ or the land height was above 1500 km. Data up to 3.5 hours either side of local midnight were also still rejected. The difference was that segments were rejected if they were less than 70% clear; a threshold of 40% clear had been previously used. This change is to take account of the fact that the water vapour channel on GOES-12 is spectrally broader than on previous instruments to allow for a finer spatial resolution.
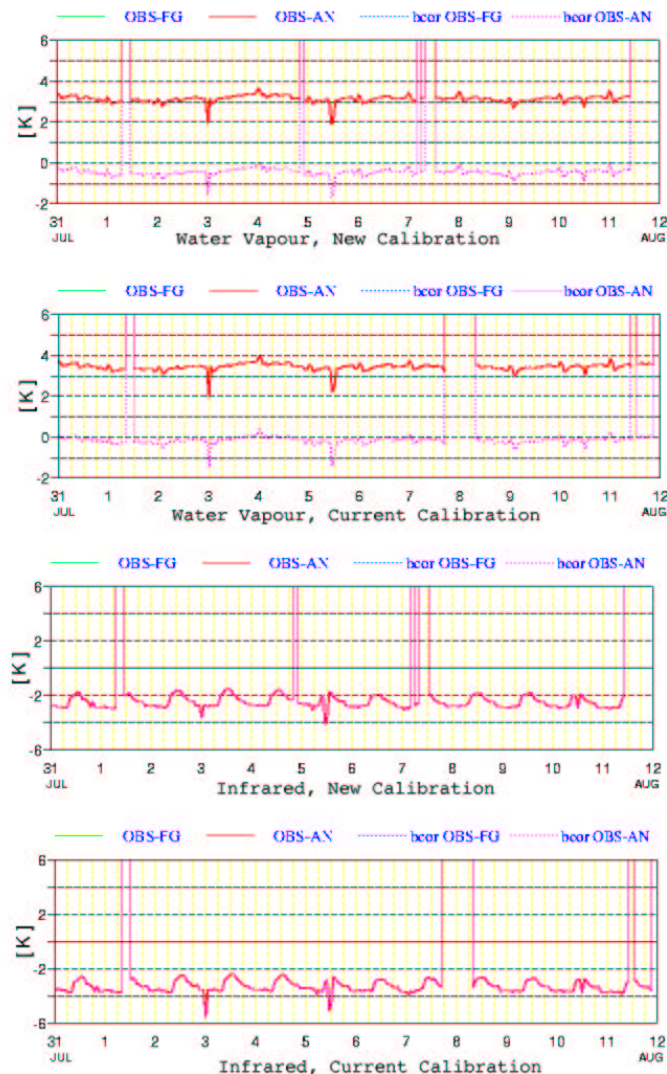
Figure 14: Mean first guess departure of Meteosat-7 water vapour and infrared radiances using current and proposed new calibrations.

The results of this experiment again show the impact on upper tropospheric geopotential height anomaly correlations to be neutral to positive, although this experiment showed a more positive result than most – see figure 22. A more detailed analysis of the 500 hPa geopotential height RMS errors (figure 23) shows a mix of positive and negative impact, with the north west Atlantic showing the most benefit.

An examination of the impact of GOES-12 assimilation on NOAA-16 HIRS-12 (figure 24) statistics is not as conclusive as the equivalent diagnostic was for Meteosat-5 assimilation (presented above), although a reduction in the standard deviation may be seen in the west Atlantic and west of equatorial South America. This is perhaps because the control experiment already assimilates similar data from GOES-10 and Meteosat-7, covering much of the GOES-12 area. It may also be indicative that further attention should be given to the bias correction of this data; the large diurnal cycle leads to a particularly challenging bias correction problem.

The results of these experiments led to the operational assimilation of GOES-12 WV CSRs. This began in IFS cycle 26r3, which was implemented operationally on 7th October 2003.
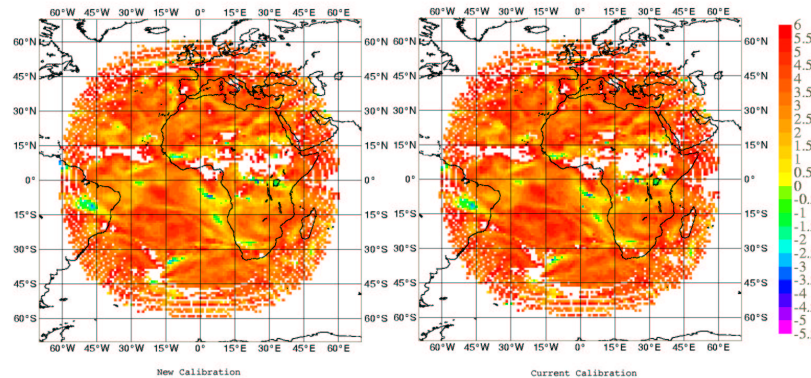
Figure 15: First guess departure of Meteosat-7 water vapour radiances using current and proposed new calibrations over the period 2200 UTC on 31st July 2003 to 0300 UTC 2nd August 2003. Note white areas denoting cloudy data.
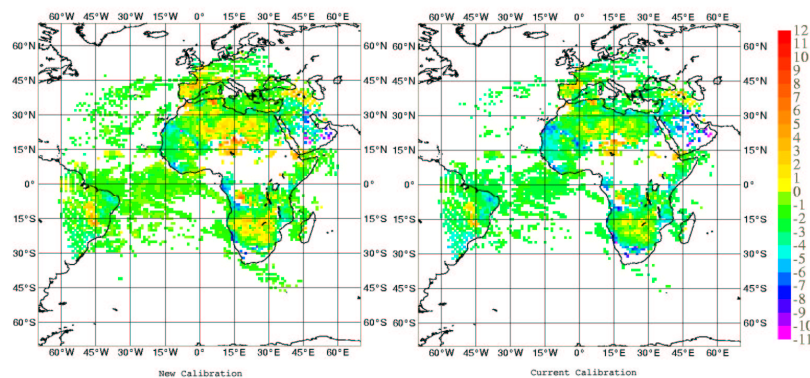

Figure 16: First guess departure of Meteosat-7 infrared radiances using current and proposed new calibrations over the period 2200 UTC on 31st July 2003 to 0300 UTC 2nd August 2003. Note white areas denoting cloudy data.

6 Assimilation of GOES-9

GOES-9 became operational over the west Pacific in May. An assimilation experiment was run for GOES-9 in a similar manner to the GOES-12 experiment above. The experiment was run over the same period, with a blacklist excluding data in the same manner. Two differences exist in the blacklist; firstly GOES-9 data are excluded for local midnight for its position over the Pacific, and secondly GOES-9 data are only excluded if the percentage of the segment found clear is 40% or less, not 70% as for GOES-12.

The results of this experiment once more show the impact on upper tropospheric geopotential height anomaly correlations to be neutral to positive – see figure 25. A full analysis of the 500 hPa geopotential height RMS errors shows a mix of positive and negative impact – see figure 26.

Analysis of the impact of GOES-9 WV CSRs on the NOAA-16 HIRS-12 statistics (figure 27) shows some reduction in the standard deviation over the GOES-9 area.

This experiment led to the operational assimilation of GOES-9 WV CSRs in IFS cycle 26r3, which was imple-
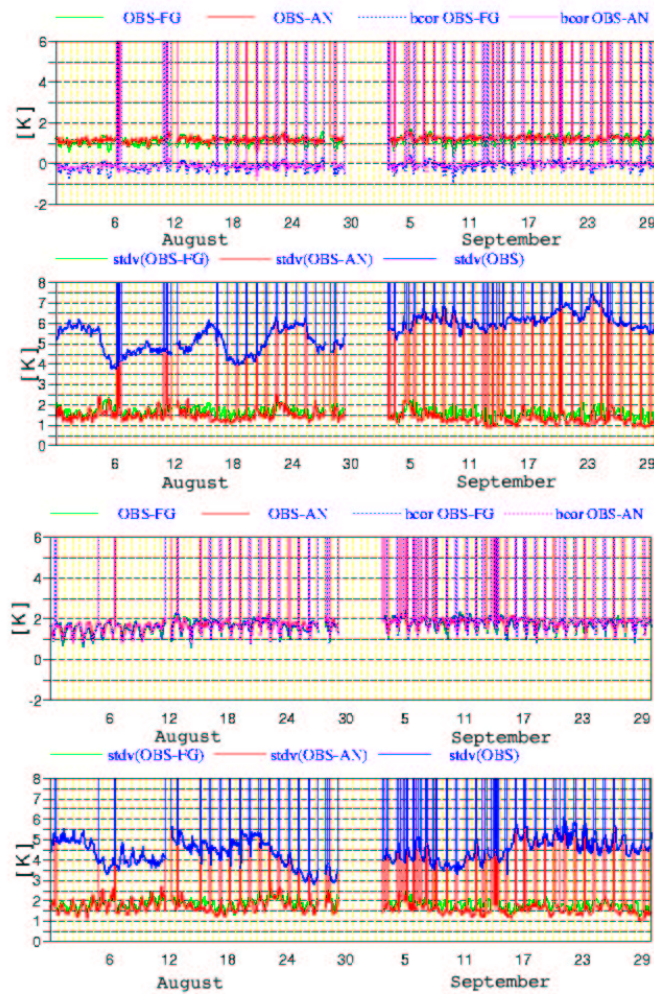
Figure 17: Mean and standard deviation of first guess departure of GOES-10 and GOES-12 water vapour channel radiances over August and September for the northern hemisphere. Top panel: GOES-10, mean. Second panel: GOES-10, standard deviation. Third panel: GOES-12, mean. Bottom panel: GOES-12, standard deviation. In the above graphs GOES-10 is being assimilated, but GOES-12 is only passively monitored.

mented operationally on 7th October 2003.

7 Geostationary radiance data denial experiment

With the introduction of IFS cycle 26R3 ECMWF assimilate clear sky radiances containing upper tropospheric humidity information at all longitudes. At the time of writing a series of observing system experiments are being run to test the impact of various data types, including clear sky radiance data. One of theses experiments, which has been completed, was run to recalculate the analyses and forecasts over July 2003 in the absence of CSR data. This was the only change in the experiment from the 'esuite' which ran over July 2003. The anomaly correlation of the 500 hPa geopotential height is shown in figure 28. This shows that the use of geostationary radiances provides a positive impact. Similar results are yielded if the 300 hPa geopotential height is studied (not shown). The t-test was used to test the significance of this result. The test was applied to northern and
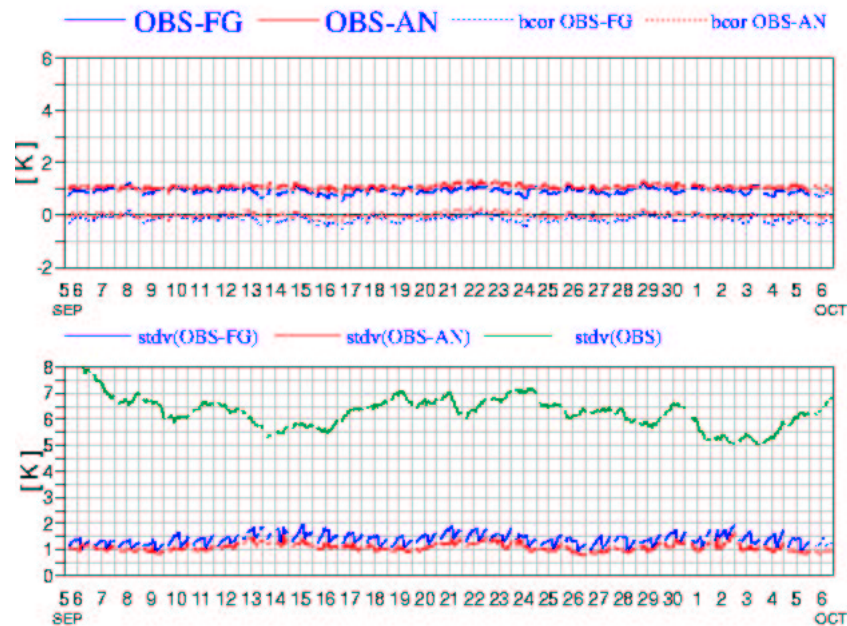
Figure 18: Mean and standard deviation of first guess departure of GOES-9 water vapour channel radiances over September for the southern hemisphere. Top panel: mean. Bottom panel: GOES-12, standard deviation. GOES-9 is being assimilated into the model used for validation here. The model used is the 'esuite' rather than operations.

southern hemisphere data at 48, 72, 96, 120, 144 and 168 hours, for both the northern and southern hemisphere, at the 10%, 5% and 1% level. A summary of the results are shown in table 1. No test showed the use of geostationary clear sky radiances to be detrimental to forecast skill.

Time	500hPa Northern Hemisphere	500 hPa Southern Hemisphere	300 hPa Northern Hemisphere	300 hPa Southern Hemisphere
48	90%	< 90%	< 90%	< 90%
72	< 90%	< 90%	< 90%	< 90%
96	< 90%	< 90%	< 90%	< 90%
120	< 90%	< 90%	< 90%	< 90%
144	90%	< 90%	< 90%	< 90%
168	95%	95%	90%	95%

Table 1: Level of significance of finding that geopotential height anomaly correlation is better for forecasts using geostationary clear sky radiance data than forecasts not assimilating these data. In the above table < 90% implies that a 90% significance t-test was failed.

An analysis of the impact of geostationary CSR assimilation on the standard deviation of NOAA-16 HIRS 12 first guess departures is shown in figure 29. The greatest reduction in the first guess departure standard deviation appears to be in areas covered by Meteosat series satellites, although some impact can be seen in the areas covered by the GOES series satellites.
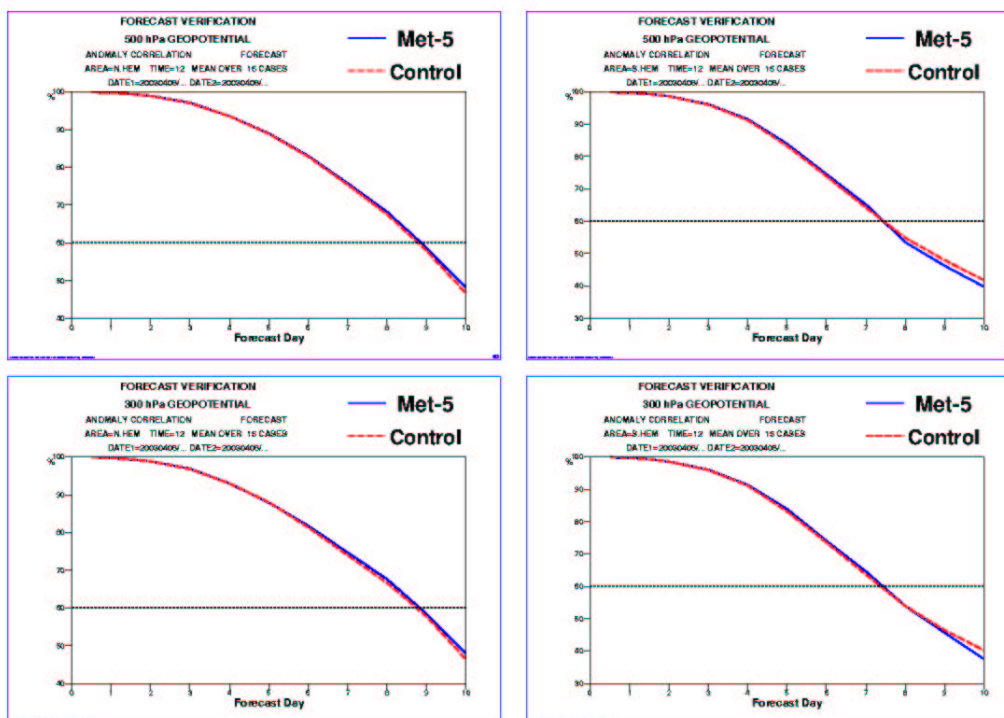
Figure 19: Geopotential height anomaly correlations for 300 and 500 hPa in the northern and southern hemisphere for Meteosat-5 radiance assimilation experiment and control. Top panels show 500 hPa and bottom panels show 300 hPa. Left panels show the northern hemisphere and right panels the southern hemisphere.

8   Summary and Future Work

Clear sky radiance data from both EUMETSAT and CIMSS continue to be monitored at ECMWF. The identification of features in the datasets inconsistent with operational assimilation has led to an evolution of these products, resulting in data able to provide a clear positive impact on forecast skill at ECMWF. This impact may be seen as 95% significant at 6 days when the 500 hPa geopotential height is used as the indicator, in both hemispheres. Furthermore the impact of the assimilation of these data may be seen in the first guess departure statistics of HIRS channel 12, showing that the moisture field is being altered in a manner consistent with other instruments.

This evolution continues, with the introduction of new instruments such as SEVIRI, new CSR datasets from existing instruments such as MODIS and improvements in the processing of current CSRs such as the fix for the GOES midnight blackbody calibration effect. All of these will be investigated in the coming months. Test SEVIRI data are now available and over the coming weeks these data will be studied passively to diagnose any remaining problems in their processing. Initial studies of the water vapour channels look encouraging, with the 7.3μm channel showing a low bias (about 0.6 K) and the two channels showing different enough structures that vertical resolution of increments should be improved. See figure 30.

The assimilation of infrared satellite data in general is hampered by the difficulty of using radiances over cloudy areas. This problem is an ongoing area of research at ECMWF, and we shall be investigating the potential of cloudy radiances from geostationary orbit.
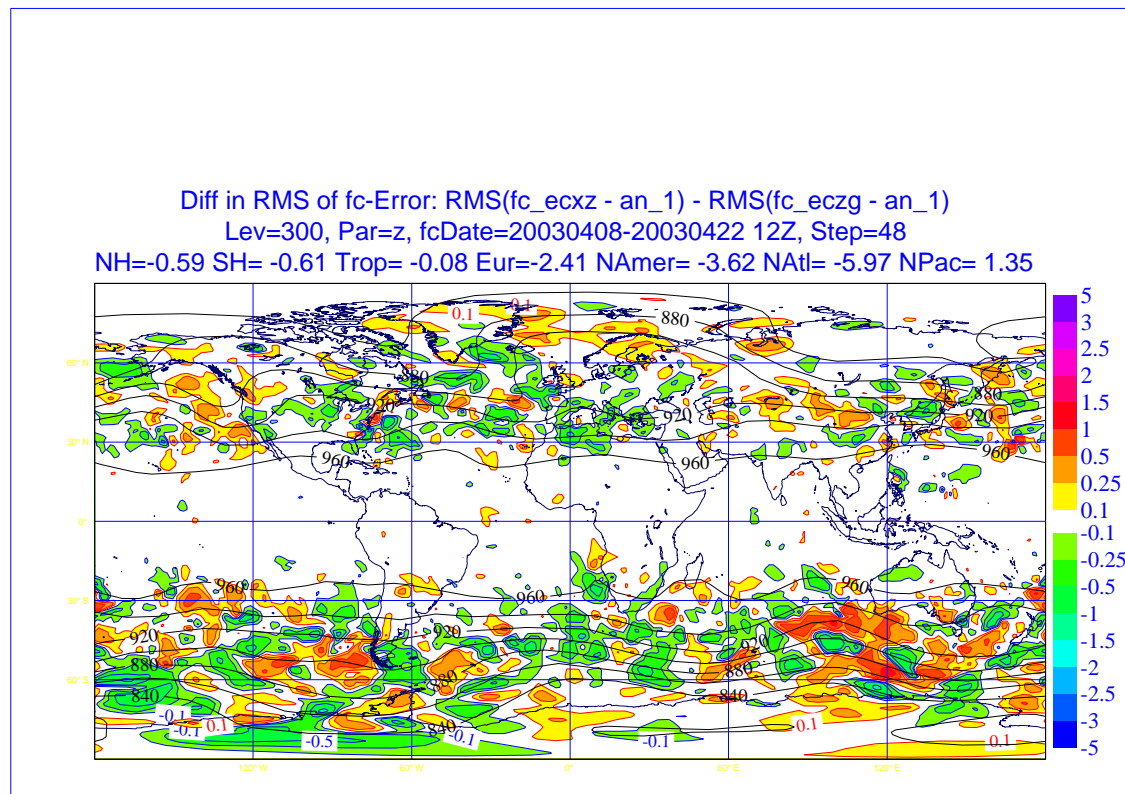
Figure 20: Difference in RMS errors in 300 hPa geopotential height at 48 hours between Meteosat-5 assimilation experiment and control.

Acknowledgments

References

Hillger, D. W., T. J. Schmit , and J. M. Daniels, 2003: Imager and Sounder Radiance and Product Validations for the GOES-12 Science Test, *NOAA Technical Report 115*, U.S. Department of Commerce, Washington, DC.

Johnson, R. X., M. Weinreb, 1996: GOES-8 imager midnight effects and slope correction. *Proceedings of SPIE conference*, 7-9 August 1996, Denver, Colorado, USA.

Köpken, C., G. Kelly, and J.-N. Thépaut, 2002: Monitoring and assimilation of Meteosat radiances within the 4DVAR system at ECMWF. *EUMETSAT/ECMWF Fellowship Report No. 9*. Available from ECMWF, Shinfield Park, Reading RG2 9AX, UK.

Köpken, C., G. Kelly, and J.-N. Thépaut, 2003: Assimilation of geostationary WV radiances from GOES and Meteosat at ECMWF. *EUMETSAT/ECMWF Fellowship Report No. 14*. Available from ECMWF, Shinfield Park, Reading RG2 9AX, UK.

Saunders, R. W., M. Matricardi, P. Brunel, 1999: An improved fast radiative transfer model for assimilation of satellite radiance observations. *Quart. J. Roy. Meteor. Soc.*, 125, 1407-1425
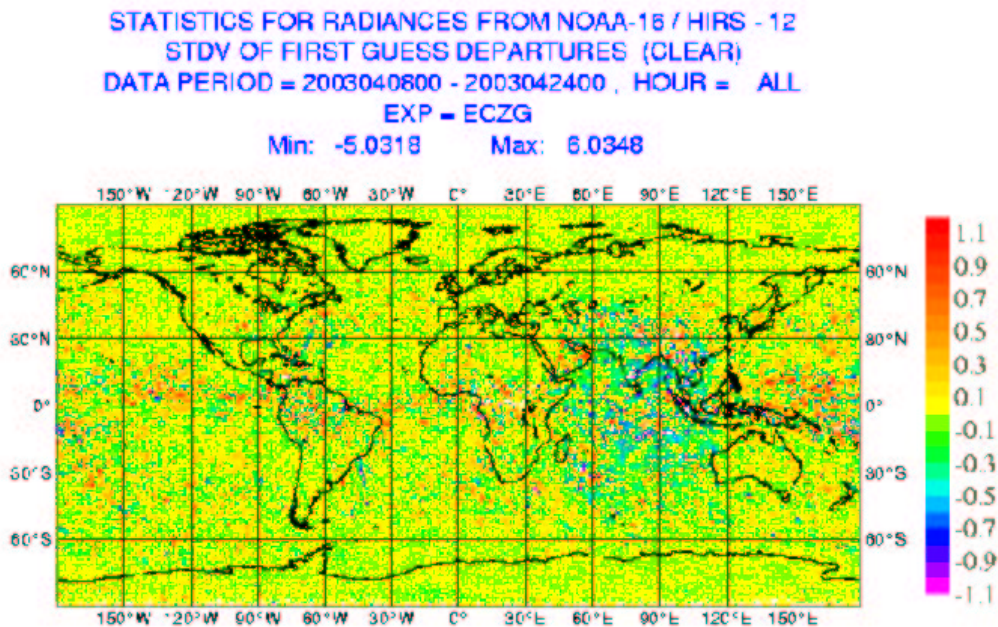
Figure 21: Difference in RMS first guess departure of HIRS channel 12 on NOAA-16 between Meteosat-5 assimilation experiment and control.
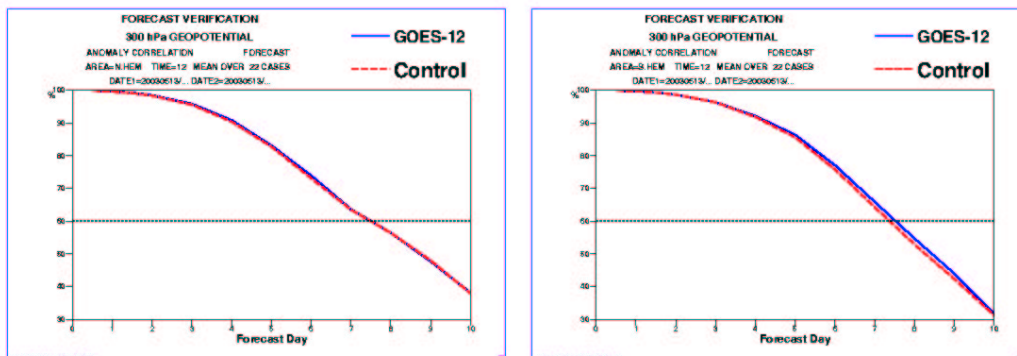

Figure 22: Geopotential height anomaly correlations for 300 hPa in the northern and southern hemisphere for GOES-12 radiance assimilation experiment and control. Left panel show the northern hemisphere and right panel the southern hemisphere.
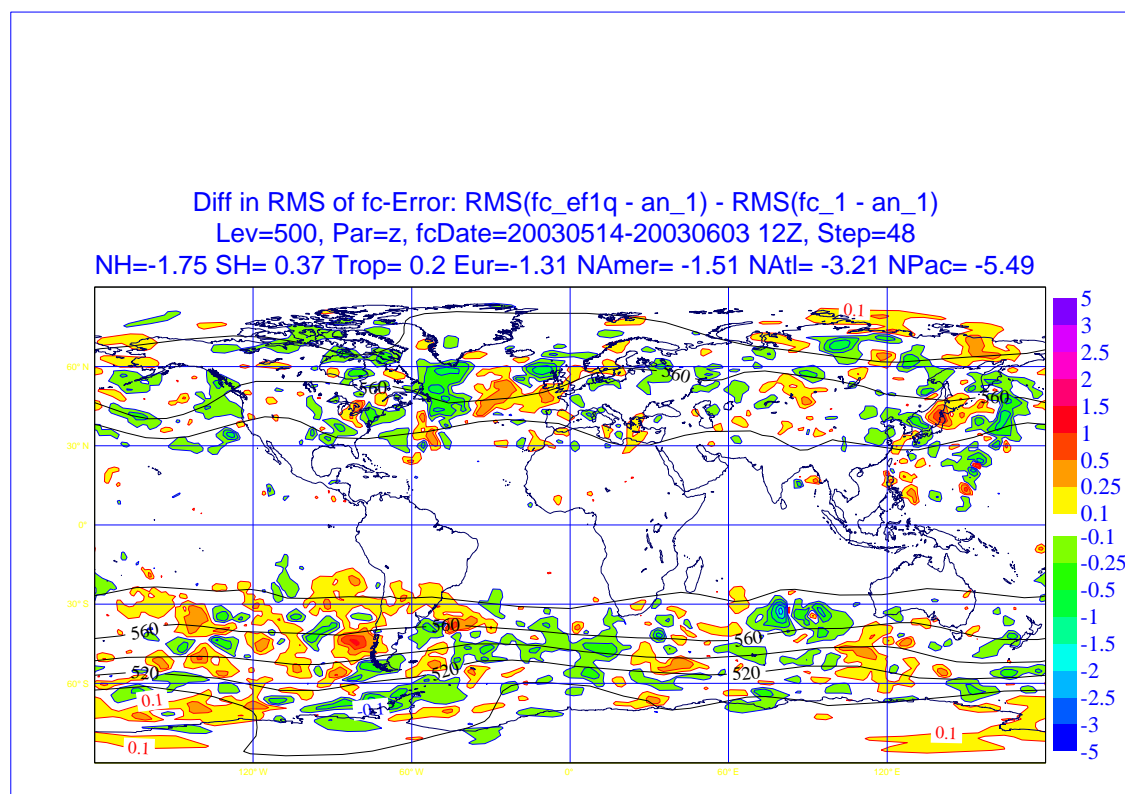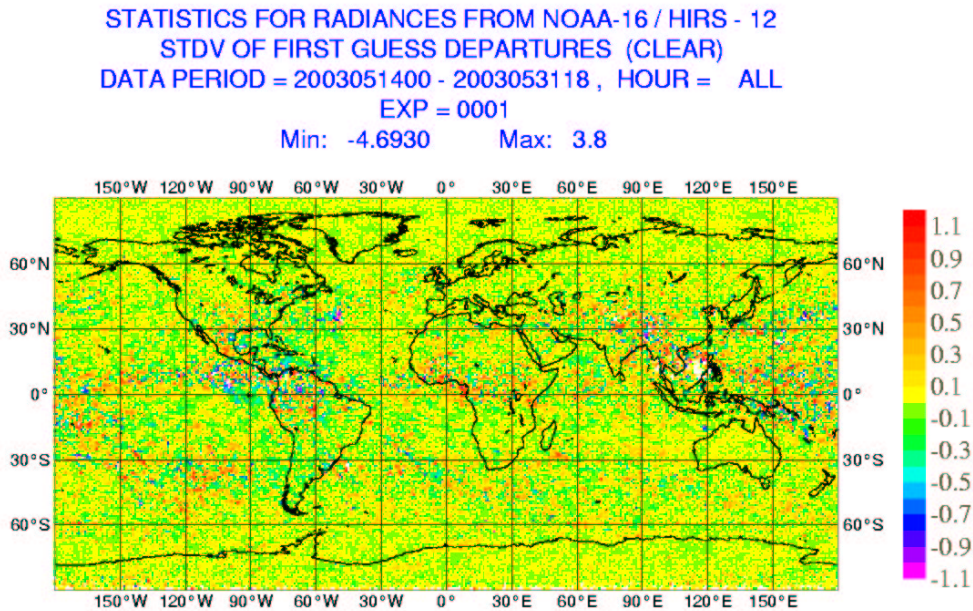
Figure 23: Difference in RMS errors in 500 hPa geopotential height at 48 hours between GOES-12 assimilation experiment and control.

Figure 24: Difference in RMS first guess departure of HIRS channel 12 on NOAA-16 between GOES-12 assimilation experiment and control.
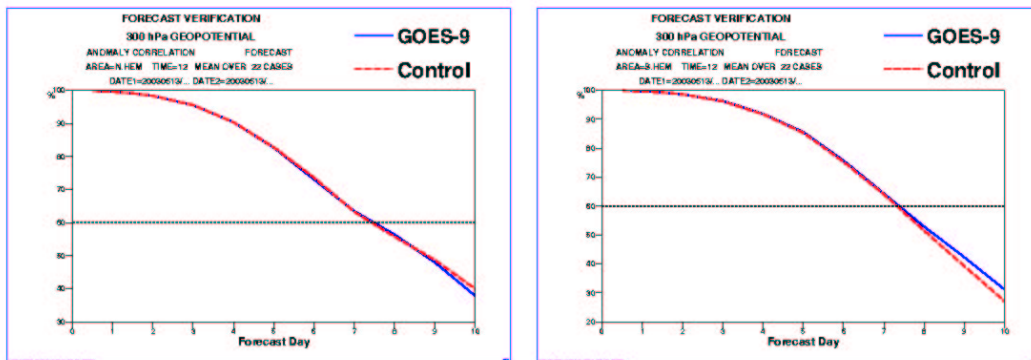

Figure 25: Geopotential height anomaly correlations for 300 hPa in the northern and southern hemisphere for GOES-9 assimilation experiment and control. Left panel show the northern hemisphere and right panel the southern hemisphere.
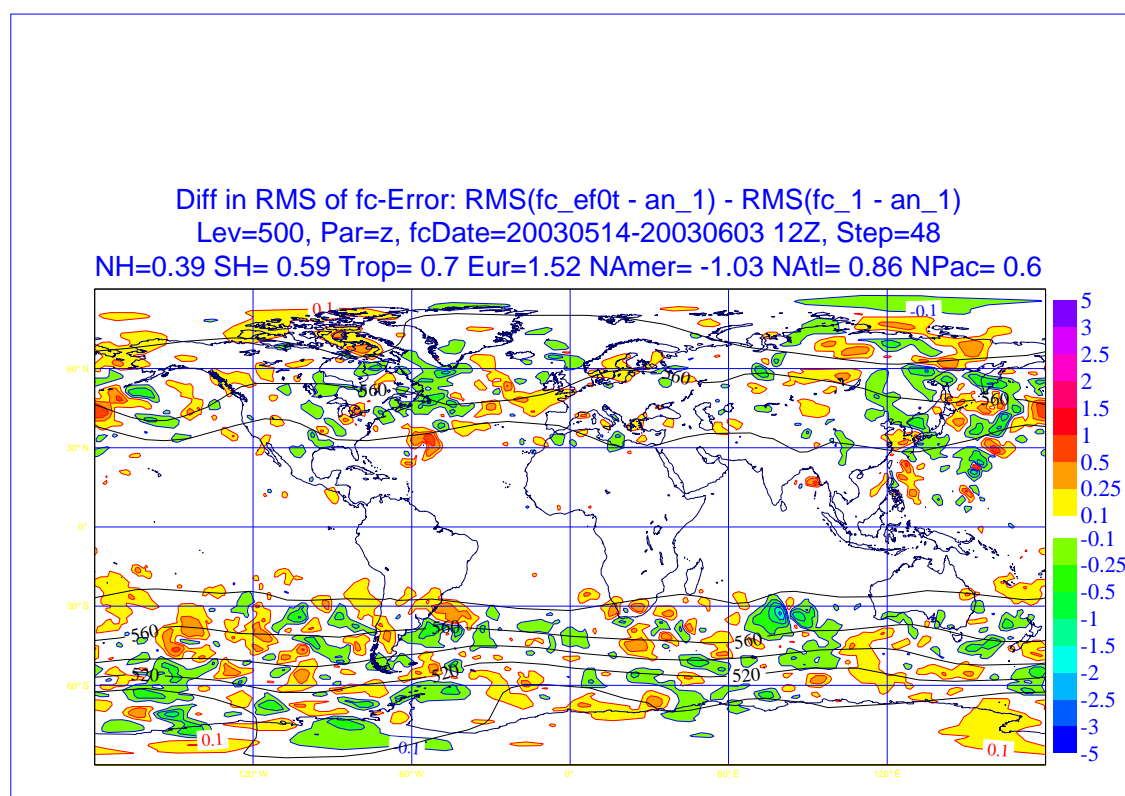
Figure 26: Difference in RMS errors in 500 hPa geopotential height at 48 hours between GOES-9 assimilation experiment and control.
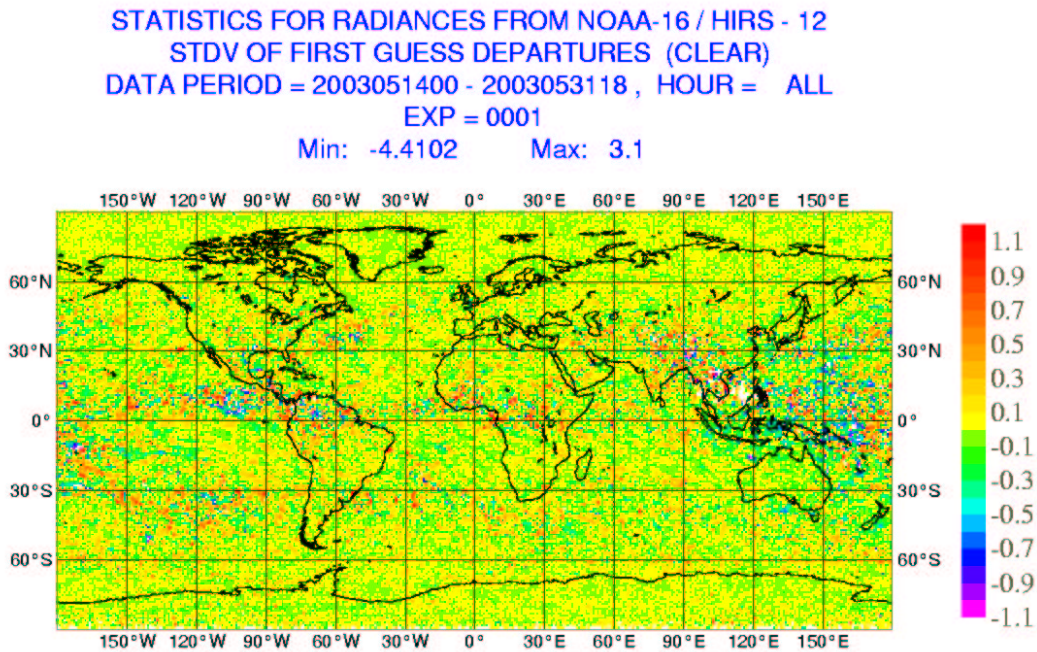
STATISTICS FOR RADIANCES FROM NOAA-16 / HIRS - 12
STDV OF FIRST GUESS DEPARTURES (CLEAR)
DATA PERIOD = 2003051400 - 2003053118 , HOUR = ALL
EXP = 0001
Min: -4.4102   Max: 3.1

Figure 27: Difference in RMS first guess departure of HIRS channel 12 on NOAA-16 between GOES-9 assimilation experiment and control.
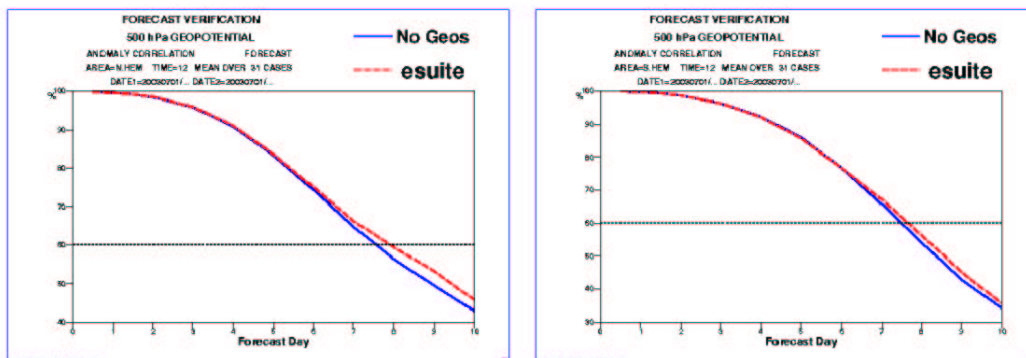
Figure 28: 500 hPa geopotential height anomaly correlations for northern and southern hemisphere (left and right panel respectively) for ECMWF IFS cycle 26R3 ('esuite') and geostationary CSR denial experiment.
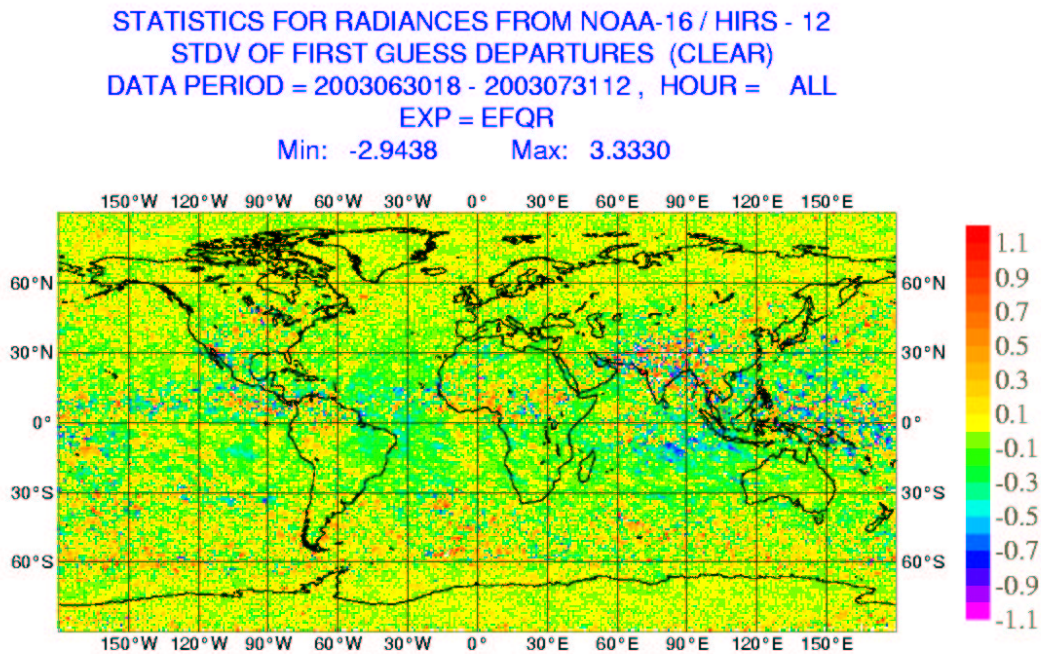
Figure 29: Difference in RMS first guess departure of HIRS channel 12 on NOAA-16 between esuite and geostationary clear sky radiance data denial experiment.
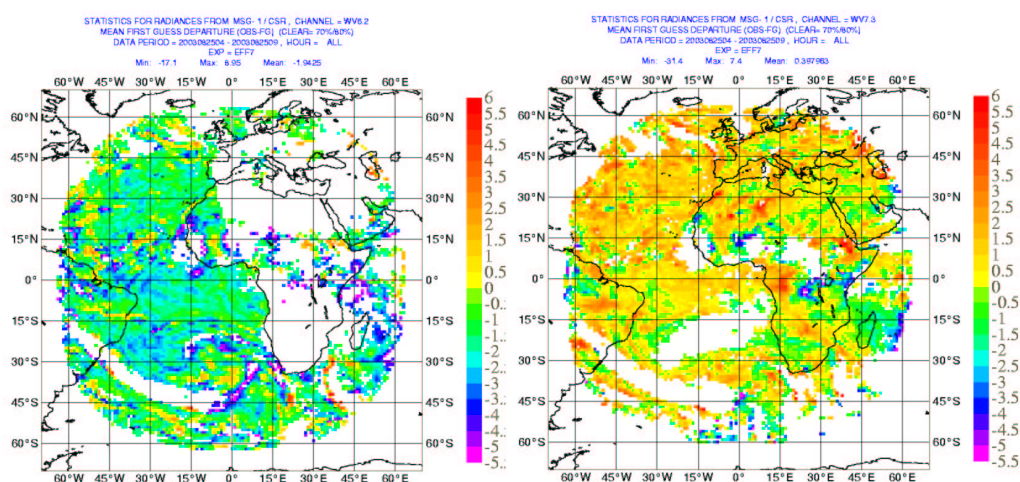

Figure 30: First guess departure of initial data for SEVIRI 6.2 μm and 7.3 μm channels (left and right panels respectively). Data for 0600 UTC on 25th August 2003.